NORTH-HOLLAND
PHYSICS
PUBLISHING

Nuclear spin weights and gas phase spectral structure of $^{12}C_{60}$ and $^{13}C_{60}$ buckminsterfullerene

William G. Harter and Tyle C. Reimer
University of Arkansas, Fayetteville, AR 72701, USA

Received 18 February 1992

Rotational energy levels and high resolution rovibrational spectra of gas phase buckminsterfullerene is strongly effected by the Pauli exclusion principle. Very different rovibrational fine structure patterns will be seen for differing arrangements of ^{13}C and ^{12}C isotopes. Only two extreme cases $^{12}C_{60}$ and $^{13}C_{60}$ actually have icosahedral symmetry. Those two cases will have relatively uncluttered spectral patterns and simpler rotational dynamics. Their analysis in turn will be a prerequisite to analyses of rotational dynamics of mixed cases. An understanding of gas phase rotational dynamics may also help to understand dynamics of icosahedral hindered rotors in the fullerite solids.

Reprinted from CHEMICAL PHYSICS LETTERS

Nuclear spin weights and gas phase spectral structure of $^{12}C_{60}$ and $^{13}C_{60}$ buckminsterfullerene

William G. Harter and Tyle C. Reimer
University of Arkansas, Fayetteville, AR 72701, USA

Received 18 February 1992

Rotational energy levels and high resolution rovibrational spectra of gas phase buckminsterfullerene is strongly effected by the Pauli exclusion principle. Very different rovibrational fine structure patterns will be seen for differing arrangements of ^{13}C and ^{12}C isotopes. Only two extreme cases $^{12}C_{60}$ and $^{13}C_{60}$ actually have icosahedral symmetry. Those two cases will have relatively uncluttered spectral patterns and simpler rotational dynamics. Their analysis in turn will be a prerequisite to analyses of rotational dynamics of mixed cases. An understanding of gas phase rotational dynamics may also help to understand dynamics of icosahedral hindered rotors in the fullerite solids.

1. Introduction

The first mass-spectroscopic evidence of an extraordinary icosahedral structure for a sixty carbon cluster was found in 1985 by Kroto, Heath, O'Brien, Curl and Smalley [1]. The proposed C_{60} molecule named buckminsterfullerene remained quite controversial [2] until it was identified using infrared spectroscopy of specially prepared carbon soot films by Krätschmer, Fostiropoulos, and Huffman [3] in 1989. Since 1972 Huffman and Krätschmer had been puzzled by the peculiar spectroscopic properties of carbon arc soot produced in a rare gas environment.

The extraordinarily high symmetry of C_{60} allows only four dipole-active (E1) infrared transitions from its vibrational ground state [4]. The infrared spectra showed two pairs of T_{1u} peaks near the values predicted by model calculations. The models also predicted a uniform frequency down shift for C_{60} molecules composed of the heavier carbon isotope ^{13}C and this shift was observed. Finally, in 1990 there were found ways to crystallize the solid C_{60} which was named buckminsterfullerite [5]. The production and distillation process was simple enough that it has been quickly reproduced and improved and allowed many workers to verify and discover new properties of C_{60} and related fullerene molecules. The combinations of infrared, Raman [6], NMR [7], X-ray [8], and STM [9,10] investigations have shown that each C_{60} cluster has the unique icosahedrally symmetric soccerball structure originally proposed.

Correspondence to: W.G. Harter, University of Arkansas, Fayetteville, AR 72701, USA.

The natural abundance of the isotope ^{13}C is 1.108% and the remaining 98.892% is ^{12}C. This means that only about half of resulting buckminsterfullerene molecules are actually $^{12}C_{60}$ with full icosahedral Y symmetry. The other half contains one or more ^{13}C nuclei. The probability for C_{60} to contain m nuclei ^{13}C is

$$p_m = \binom{60}{m} (0.01108)^m \, (0.98892)^{60-m} . \qquad (1)$$

Even a single ^{13}C completely destroys the rotational symmetry since the atomic sites are not located on symmetry axes. An extra neutron has only a small effect (≈ 1 cm^{-1}) on the gross vibrational spectral structure of solid C_{60}. However, the detailed rotational vibrational fine structure of gas phase C_{60} will be very sensitive to even a single replacement of a ^{12}C by ^{13}C. Also, ^{12}C has a spin-0 nucleus while ^{13}C has a spin-1/2 nucleus. Therefore the Pauli-allowed spin-rotation states of C_{60} become increasingly complicated as more of ^{12}C are replaced by ^{13}C nuclei.

This also affects the nuclear spin statistical weights and the hyperfine structure of high resolution spectra.

In this paper, we will discuss and compare the possible nuclear spin rotation states and spectra for the two extreme cases of buckminsterfullerene which still have icosahedral symmetry. The first case $^{12}C_{60}$ is totally made of ^{12}C and the second case $^{13}C_{60}$ is all ^{13}C. We are presuming that it will be possible to obtain graphite or carbon samples that are somewhat better than 1% pure ^{12}C for the first case, and that reasonably pure ^{13}C samples will be available as well Furthermore, we are presuming that either of these two samples can be used for synthesis of $^{12}C_{60}$ or $^{13}C_{60}$. It should be possible to obtain enough of either material to be able to carry out gas phase Fourier transform, laser diode, or saturation absorption spectroscopy, and that these samples can be cooled in nozzle or slit expansion chambers .

So far, the gas phase spectra of C_{60} even at the resolution of Fourier transform spectroscopy has been extraordinarily congested [11]. Two of the reasons for this congestion are controllable. First, low lying H_g fundamentals are excited at room temperature and this gives rise to hot bands. Second, the use of carbon which has naturally abundant mixtures of ^{12}C and ^{13}C yields a panoply of complex and different spectral patterns.

In order to assign high resolution spectra of C_{60} it will help greatly to begin with $^{12}C_{60}$ which, as we will show, has a very simple rotational and fine structure patterns because of the Pauli exclusion principle. The material must be isotopically pure enough that its simple spectral patterns are not obscured by the more complicated patterns arising from molecules which contain ^{13}C. Adjusting eq. (1) shows that if 99.5% pure ^{12}C samples are used then 74% of the molecules are $^{12}C_{60}$. ^{12}C purity of 99.9% yields 94% pure $^{12}C_{60}$. More complicated spectral patterns will arise from mixed isotopic $^{12}C_{60-m}$ $^{13}C_m$ molecules even for small number ($m=1, 2, ...$) of ^{13}C nuclei which occur in natural populations. Furthermore, mixed isotopic species with a fixed value of m will not be easy to produce, and for $m \geqslant 2$ the steric placement of ^{13}C nuclei will be even less under experimental control.

Therefore, the next step in C_{60} high resolution spectroscopy (after assigning $^{12}C_{60}$ bands) should involve the isotopically purified $^{13}C_{60}$. The degree of purification of $^{13}C_{60}$ may not have to be as high as that of $^{12}C_{60}$ which has most of its rotational spectral structure removed by Pauli exclusion. By contrast the $^{13}C_{60}$ molecule has astronomically high spin statistical weights, as we will show. However, it will be necessary to avoid having a majority of spectral contributions from mixed species $^{12}C_{60-m}{}^{13}C_m$. Successful assignment of spectra for the latter will be difficult unless one has molecular constants obtained from spectra of $^{12}C_{60}$ and $^{13}C_{60}$.

Accurate rotational and rovibrational modeling of gas phase C_{60} systems may be relevant to better understanding of crystalline fullerite behavior. There is evidence that the buckyballs rotate rather easily in their lattice sites. Apparently, the rotation persists even as the lattice is cooled to quite low temperatures. Theory of the weakly hindered icosahedral rotor would contain some of the aspects of gas phase theory. Indeed, the gas phase rotational analysis probably needs to be done first since it is simpler and more controllable.

The rotational degrees of freedom may be an important part of the low energy lattice dynamics of fullerites and doped fullerite structures. There has never been a crystal made of a molecule that is so nearly spherical. Also, it is the first substance to host a lattice of alkali atoms and make a superconductor. While seeking a theory for fullerite–alkali superconductivity one should not ignore any possible coupling mechanisms such as collective rotation–vibrations of the carbon clusters. The presence of ^{13}C isotopes might affect the low energy fullerite lattice dynamics if C_{60} rotations were involved.

2. Spin-permutation symmetry of $^{12}C_{60}$

Spin zero ^{12}C nuclei are bosons and are restricted by the Pauli exclusion principle to have only A-type spin states and corresponding A-type rotational wavefunctions. The rotational angular momentum J quantum values which are correlated [12–14] with A for $J<30$ are $J=1$, 6, 10, 12, 15, 16, 18, 20, 21, 22, and 24–28. The others are excluded. Spectral lines based upon the excluded levels would be absent.

Fig. 1 shows sketches of hypothetical infrared rovibrational spectra for a fundamental ($0\rightarrow1$) transition for one of the four T_1-type modes [12–14]. The P and R branches of the $^{12}C_{60}$ spectrum around the

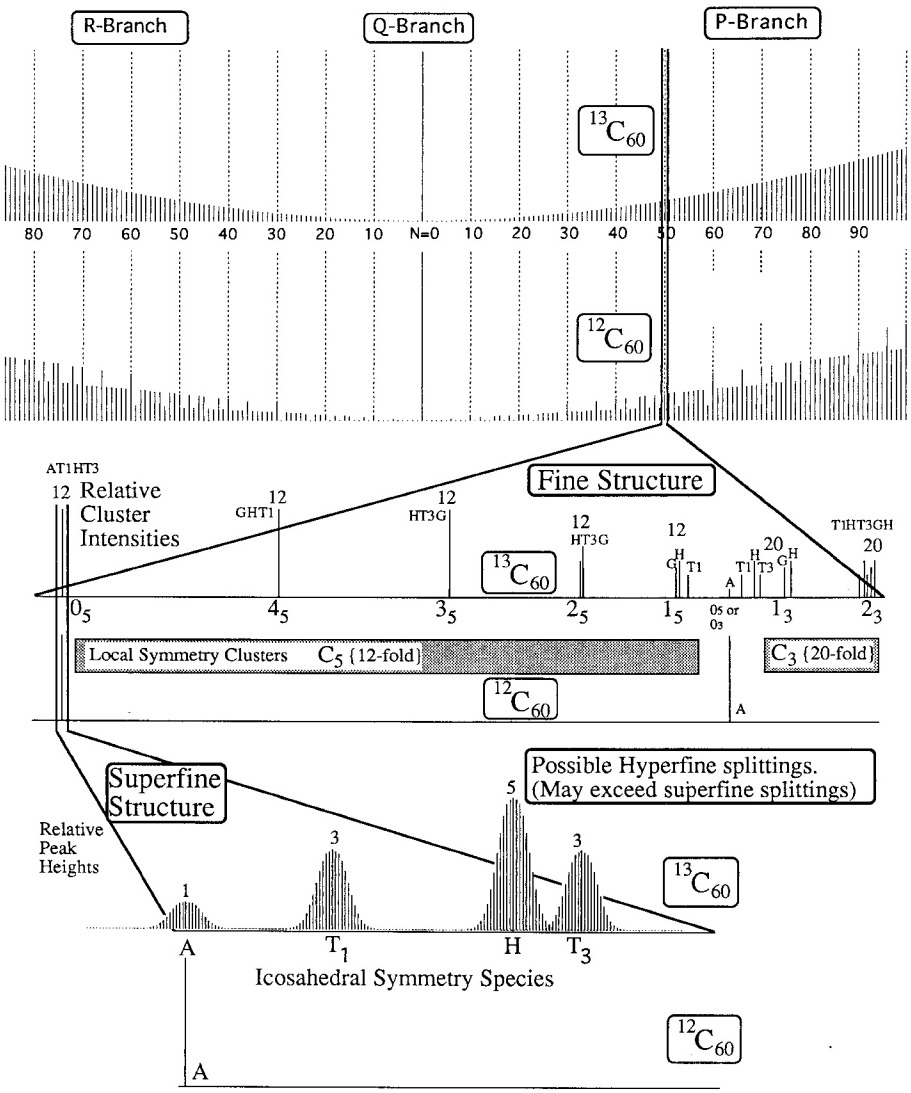

Fig. 1. Possible rovibrational structure of an infrared active T_{1u} fundamental of C_{60}. (IR fundamentals exist at 528, 577, 1183, and 1429 cm^{-1}.) (a) Rotational structure should be mostly uniform splitting in the P and R branches with spacings of $2B(1-\xi)=0.0064$, 0.0086, 0.0076, and 0.0062 cm^{-1}, respectively, for each of the four fundamentals (see ref. [15]). (b) Fine structure splitting varies as the sixth or higher powers of angular momentum $R=N$ or J and could range between a few kHz and several GHz. $^{12}C_{60}$ has only O_5 and O_3 peaks (see ref. [13]). (c) Superfine splittings vary exponentially over many orders of magnitude from virtually nothing to several MHz. $^{12}C_{60}$ has only A species (see ref. [13]). (d) Hyperfine splittings for $^{13}C_{60}$ would vary linearly with angular momentum J and nuclear spin I ($0<I\leqslant 30$) and could be several kHz. $^{12}C_{60}$ has no hyperfine structure at all.

Q branch show the gaps that result from the Pauli exclusion principle. Only lines R(0), R(6), R(10), R(12), R(15), ..., R(28) (or P(6), P(10), P(12), P(15),..., P(28)) can appear. The notation R(J) means rotational momentum is raised from J to $J+1$ in the transition while P(J) means it plunges from J to $J-1$. So each R(J) and P(J) line reflects the ground state J population. Each J level has its Boltzmann population factor $\rho_J \exp(-\beta E_J)/Z$. The Boltzmann factor is shown rising as it would near room

temperature (300 K). However, if the molecules were cooled sufficiently (≈ 10 K) the population could be concentrated into just the lowest allowed J values of 0, 6, 10, 12, ... Even a moderate cooling would also reduce hot band transitions arising from thermally excited vibrations and return population from these levels to the purely rotational levels [15].

At higher temperatures the levels with higher J become populated. For C_{60} at room temperature the most populated levels have hundreds of rotational quanta which in turn correspond to thousands of angular momentum sublevels. The detailed quantum mechanics of high $-J$ rotational levels and their $(2J+1)$-dimensional manifold of sublevels can be simplified using semiclassical models [12,13]. For the purely bosonic fullerene $^{12}C_{60}$ the Pauli exclusion principle leads to a further simplification of the quantum states and levels. Only one out of sixty rotational substates survives the symmetry exclusion.

Centrifugal and coriolis distortion of spherical top molecules is known to split J levels into multiplets labeled by symmetry species. At high J these multiplets tend to form clusters. These are analogous to clusters observed in SF_6 [16–19], which is an octahedral analog of C_{60}. An example of a hypothetical $J=50$ level splitting for C_{60} P(50) is sketched in fig. 1. Using the lowest order centrifugal distortion tensor Hamiltonian one predicts spectral structure such as is displayed in the lower half of fig. 1. At the extreme left hand side of fig. 1 there is a magnified view of a 0_5 cluster of icosahedral species A, T_1, H, T_3 which together would contain twelve $(1+3+5+3=12)$ rotational sublevels if they were Pauli-allowed. For $^{12}C_{60}$ only the A sublevel is allowed. The next cluster to the right is labeled 4_5 and also has twelve levels but different symmetry species G, H, and T_1. However, all of these are Pauli-excluded in a $^{12}C_{60}$ spectrum.

Each cluster in fig. 1 is labeled by an approximate quantum number k_5 or k_3. This is related to the azimuthal component of the angular momentum on body axes of fivefold (C_5) or threefold (C_3) symmetry respectively. The 0_5 levels correspond to states with rotational quanta of $K=50$ around each of twelve C_5 symmetry axes and are labeled 0_5 since $50=0$ mod 5. The neighboring 4_5 cluster corresponds to twelve nearly degenerate states of $K=49=4$ mod 5 and similarly for 3_5, 2_5, ..., which label clusters to the right. At the extreme right hand side is a cluster of states with $K=50=2$ mod 3 which is better described by C_3 symmetry. It corresponds to an angular momentum of $K=50$ around C_3 axes, and is labeled 2_3 since $50 = 2$ mod 3. It contains twenty rotational sublevels, exactly the number of C_3 axes in C_{60}, distributed amongst the Y species T_1, H, T_3, G, and H. The qualitative species ordering and clustering of levels and clusters may be found using fig. 2. However, 2_3 ($K=50$) and 1_3 ($K=49$) clusters in the $J=50$ manifold are Pauli-excluded for $^{12}C_{60}$. The 0_3 cluster is close to the boundary between C_3 and C_5 clusters.

For $^{12}C_{60}$ all clusters are empty except those of 0_3 or 0_5 symmetry which contain a single A line. The A line sits where it would have been if all the other species were present. The $J=50$ example has only two such lines. The other ninety-nine substates are excluded. A second A line lies in what is called the separatrix region between the C_5 and C_3 cluster ladders. This peak is indicated in the lower center portion on the right hand side of fig. 1. Directly above it is an At line in the corresponding spectrum of $^{13}C_{60}$ which is discussed later. Each A line in the $^{12}C_{60}$ spectrum has sixty times the intensity it would have had if all species were Pauli allowed.

Indeed it may seem futile to discuss level clusters

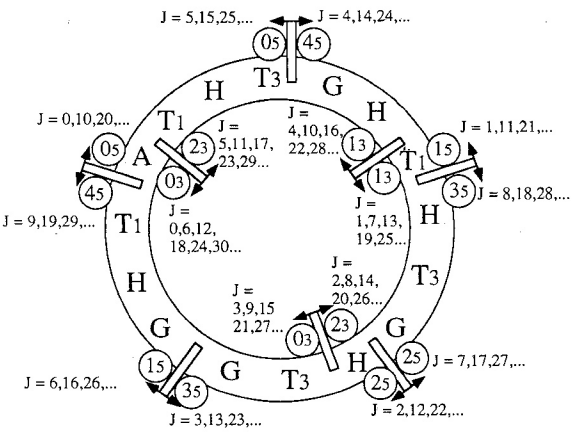

Fig. 2. Cycle diagram for fine and superfine structure for $J=0$–29. (The cycle repeats for $J=30+j$ which has the same species as $J=j$ plus a complete regular sequence.) Species for a given J level are enclosed by arrows labeled by that value of J and are ordered as they appear in the ring. The cluster quantum numbers are enclosed in small circles.

for $^{12}C_{60}$ in which practically all the states are missing. However, the physical properties of the rotational wavefunctions for the allowed states in $^{12}C_{60}$ would be identical to the corresponding ones in $^{13}C_{60}$. The difference is that the $^{13}C_{60}$ spectrum has all the species needed to make a superfine structure and this gives a direct measurement of the localization of the corresponding rotational states [12,13]. For example, the small A line for $^{13}C_{60}$ is one of several lines between the C_5 and C_3 bands and lies directly above an isolated A line for $^{12}C_{60}$ in fig. 1. The $^{13}C_{60}$ A line clearly falls in a region where lines are not clustering. It is clearly distinguished from the first A line in $^{13}C_{60}$ which is clustered with eleven other species. By contrast the $^{12}C_{60}$ spectrum has just two A lines and no obvious way to distinguish them.

Each A line in the $^{12}C_{60}$ spectrum belongs to a totally symmetric nuclear spin-0 state which is the only state sixty spinless nuclei can make. All the nuclear angular momentum in $^{12}C_{60}$ comes from rotational or vibrational motion of the nuclei.

3. Spin-permutation symmetry of $^{13}C_{60}$

Sixty spin-1/2 nuclei yield an enormous number ($2^{60}=1.2\times10^{18}$) of spin states. (By comparison, the analogous SF_6 molecule has only 64 spin states [16–18].) Each state can have one of thirty-one different values of total nuclear spin quanta ranging from $I=0$ to $I=30$ in unit steps. The $^{13}C_{60}$ molecule has large nuclear spin I as well as large rotor momentum R or J. A given spin state is associated with an orbital or rotational state of definite icosahedral symmetry species A, T_1, T_3, G, or H if and only the resulting product makes a Pauli-allowed state that is totally antisymmetric to permutations of the sixty ^{13}C nuclei. While icosahedral symmetry Y is formidable compared to most molecular point groups it is tiny compared to the overlying permutational symmetry S_{60} of C_{60} which has 60! elements, or approximately 8.32×10^{81} permutations.

Fortunately, the mathematics of permutation symmetry and the related unitary groups contains some powerful computational methods [17,19–21]. Various formulas based upon Young tableaus make it relatively easy to compute characters and irreducible representations of large symmetric and unitary groups. Here Coleman's character formula is used to compute S_{60} characters for icosahedral classes in order to deduce the $S_{60}\supset Y$ correlation table. This is analogous to the S_6 permutational analysis of SF_6 given in ref. [16,17].

For sixty spin-1/2 nuclei ^{13}C we need only the S_{60} spin tableau $[\mu_1, \mu_2]$ which have at most two rows. Each nucleus has only two spin states to put in a column of a tableau. Since tableau columns represent antisymmetrized combinations there can be at most two rows in each. Any column containing two or more identical spin states nullifies that entire tableau state.

An allowed $^{13}C_{60}$ spin-1/2 tableau $[\mu_1, \mu_2]$ will have sixty boxes each containing spin up or spin down according to the value of each individual nuclear spin. Each tableau has μ_1 boxes in its first row and μ_2 boxes in its second which is always less than or equal to the length of the first row ($\mu_1\geqslant\mu_2$). The sum of the row lengths is the number of boxes or the number of nuclei which is sixty ($\mu_1+\mu_2=60$). Each box in the second row corresponds to an antisymmetrized pair involving itself and the one above so there are μ_2 scalar pairs in a $[\mu_1, \mu_2]$ tableau state. The remaining $(\mu_1-\mu_2)$ boxes represent unpaired nuclei that can each contribute 1/2 to the total spin angular momentum I of the $[\mu_1, \mu_2]$-tableau state.

$$I=\tfrac{1}{2}(\mu_1-\mu_2)\,, \quad \text{where} \quad \mu_1+\mu_2=60\,. \tag{2}$$

The preceding equations determine which total nuclear spin states $I=0, 1, 2,..., 29, 30$ belong to each of 31 allowed tableaus.

Each allowed tableau gives a set S_{60} characters $\chi^{[\mu_1\mu_2]}_{\alpha_1\alpha_2...}$ for each of the five classes of Y or each of ten classes of Y_h. The cycle structure $\{\alpha_1\alpha_2...\}$ of each icosahedral class depends upon how a C_{60} symmetry operation permutes the nuclei. A model of the C_{60} fullerene structure helps to visualize its S_{60} cycle structure. α_1 is the number of nuclei that are unchanged. α_2 is the number of pairs of nuclei that transposed into each others' locations. α_3 is the number of nuclear three-somes that get cycled into each others' original locations, and so forth. For example, a 120° rotation of C_{60} has twenty 3 cycles while a 72° rotation has twelve 5 cycles. This is denoted 3^{20} and 5^{12}, respectively. The general cycle notation is $1^{\alpha_1}\,2^{\alpha_2}\,3^{\alpha_3}...n^{\alpha_n}$ for a S_n class of cycle structure $\{\alpha_1\alpha_2...\alpha_n\}$.

The frequency f^{ρ} of each icosahedral representation $\rho = A, T_1, T_3, G$, and H in a given tableau $[\mu_1\mu_2]$ representation of S_{60} is calculated using the characters $\chi^{[\mu_1\mu_2]}_{\alpha_1\alpha_2\ldots}$ and icosahedral characters χ^{ρ}_{α} of Y-class α

$$f^{\rho}[\mu_1\mu_2] = \tfrac{1}{60} \sum_{\alpha} \chi^{[\mu_1\mu_2]}_{\alpha_1\alpha_2\ldots}\chi^{\rho}_{\alpha} . \qquad (3)$$

The same formula applies to classes of the full icosahedral group Y_h. The frequencies of Y_h irreps belonging to each allowed S_{60} tableau $[\mu_1\mu_2]$ and corresponding total nuclear spin $I = \frac{1}{2}(\mu_1 - \mu_2)$ are given in table 1.

Each column of this table tells how many of each hyperfine multiplet belongs to a particular icosahedral symmetry species ρ. For example, $\rho = A_g$ has just one $I = 30$ multiplet while A_u has none. Neither A_g nor A_u has an ($I = 29$) multiplet but they have 33 and 3 ($I = 28$) multiplets, respectively. The other icosahedral species fail to produce any ($I = 30$) multiplets but have several belonging to $I = 29$ and several hundred belonging to $I = 28$.

For nuclear spin values below $I = 27$ or 28 the number of possible spin states belonging to each icosahedral species A, T_1, T_3, G, or H increases exponentially. It exceeds ten trillion states for each of the species with $I = 10$. Then the numbers of states begin to level off and attain a maximum value of about one hundred and fifty trillion for H_u or H_g species having nuclear spin $I = 3$ and 4. The number of H_u or H_g states with $I = 2$, 1, and 0 is, respectively, about six hundred and fifty, four hundred and fifty, and one hundred and fifty trillion. By comparison, there are only a handful (a few hundred billion) of states with $I = 16$ or greater. They probably will be difficult to see if all states are evenly populated.

The spectral profile belonging to a given species consists of a bell shaped distribution of hyperfine lines as sketched in fig. 3. Hyperfine states having a given I value will contribute $2I + 1$ spectral components split more or less evenly around the center of each distribution. The lowest I values ($I < 10$) account for the bulk of the total line intensity. Greater I values correspond to hyperfine components split across a wider range, but there are fewer of them. In figs. 1 and 3 we are assuming the simplest case in which the superfine splitting is large enough to resolve features belonging to single icosahedral species A, T_1, T_3, G, or H. (This is called hyperfine case (1) in ref. [16].) The hyperfine components are grouped into equally spaced lines as they would appear if split by the simplest scalar $\boldsymbol{I}\cdot\boldsymbol{J}$ spin rotation interaction. The height of a line located I spaces from the center of the bell shaped A pattern is proportional to the sum of numbers in the A column of table 1 belonging to all spins less than or equal to I. The center line height is the sum of the entire A column. T_1, T_3, G, or H hyperfine patterns are plotted in this way, too.

If individual icosahedral multiplet patterns can be resolved they will have an identifiable set of relative intensities as indicated in fig. 1. Each spin component and the sums thereof will contribute intensity in approximately the ratio 1:3:3:4:5 for species A, T_1, T_3, G, and H, respectively. This is true for either parity g or u. This ratio is closely followed by numbers in the rows of table 1 below $I = 25$ or 26. This approximation becomes better as I decreases but breaks down completely for the highest values of $I =$ 30, 29, or 28. However, the latter only account for a few hundred states.

Indeed, it is extraordinary to have nuclear spin weights that mirror the *rotational* degeneracies of the molecular symmetry. This is not the case in most other high symmetry molecules such as SF_6. The extraordinary weights occur because most of the allowed C_{60} nuclear spin states belong to a regular representation of icosahedral symmetry for which the repetition number of each irreducible representation is equal to its dimension. A regular representation is the primitive induced representation induced by the unit subgroup C_1. It describes the symmetry of most of the primitive spin states since each nucleus sits on a site of C_1 symmetry. The rare spin arrangements which have higher symmetry and belong to a smaller induced representation give differing ratios for species A, T_1, T_3, G, and H. However, from the tables it is evident that special spin states represent less than one in a hundred thousand. Such small discrepancies are probably well below the error of experimental intensity measurements. They would require the very highest resolution studies of individual components of hyperfine structure in the wings of the distributions.

Since most of the nuclear spin multiplets $I = 0$, 1, 2, ... contain icosahedral species {A, T_1, T_3, G, H} according to the regular ratio of 1:3:3:4:5 it follows

Table 1
Frequency table relating the number of Y_h species {A, T_1, T_3, G, H} that correlate with each of the S_{60} permutation group species. The g and u characters in the parity column denote even and odd parity respectively, and the *I* column labels each of the pertinent S_{60} species by total nuclear spin

I	Par	A	T_1	T_3	G	H
30	g	1	0	0	0	0
	u	0	0	0	0	
29	g	0	1	1	2	3
	u	0	2	2	2	2
28	g	33	39	39	57	75
	u	3	39	39	57	75
27	g	269	801	801	1085	1359
	u	271	829	829	1085	1331
26	g	4046	11282	11282	15110	18950
	u	3612	11280	11280	15110	18950
25	g	41368	124214	124214	165794	207380
	u	41426	124592	124592	165794	207002
24	g	374239	1114564	1114564	1486779	1858893
	u	370207	1114536	1114536	1486779	1858921
23	g	2800261	8402446	8402446	11204737	14007123
	u	2801045	8405722	8405722	11204737	14003847
22	[illegible]					

These results have errors. See Errata pages for correct spin weights

21	g	101864314	305606234	305606234	407484250	509361698
	u	101871244	305626708	305626708	407484250	509341222
20	g	505177959	1515255954	1515255954	2020362627	2525469903
	u	505038729	1515252678	1515252678	2020362627	2525473179
19	g	2227510875	6682621110	6682621110	8910203271	11137785399
	u	2227555101	6682719390	6682719390	8910203271	11137687119
18	g	8805851010	26416404008	26416404008	35221958130	44027509830
	u	8805277710	26416383532	26416383532	35221958130	44027530305
17	g	31395687995	94187500418	94187500418	125583485280	156979472565
	u	31395905010	94187877158	94187877158	125583485280	156979095825
16	g	101493183420	304475675220	304475675220	405967840740	507460006260
	u	101491245900	304475576940	304475576940	405967840740	507460104540
15	g	298734243464	896204426050	896204426050	1194939687304	1493674940916
	u	298735095224	896205610090	896205610090	1194939687304	1493673756876
14	g	803455855928	2410356623278	2410356623278	3213809552854	4017262490072
	u	803450379744	2410356246538	2410356246538	3213809552854	4017262866812
13	g	1980108752872	5940331748258	5940331748258	7920443427592	9900555106928
	u	1980111497692	5940334856362	5940334856362	7920443427592	9900551998822
12	g	4481740748565	13445195980095	13445195980095	17962929575085	22408663150695
	u	4481727625455	13445194796055	13445194796055	17962929575085	22408664334735
11	g	9331433106795	27994314140265	27994314140265	37325754400635	46657194680385
	u	9331440507045	27994321047165	27994321047165	37325754400635	46657187773485
10	g	17892036456278	53676055494765	53676055494765	71568076928288	89460098362058
	u	17892009519368	53676052386660	53676052386660	71568076928288	89460101470162

Table 1
Continued

I	Par	A	T_1	T_3	G	H
9	g	31605164625728	94815527682480	94815527682480	126420707330962	158025886940438
	u	31605181547632	94815540805590	94815540805590	126420707330962	158025873817328
8	g	51415150876770	154245357228270	154245357228270	205660480791390	257075604393270
	u	51415103156370	154245350321370	154245350321370	205660480791390	257075611300170
7	g	76925412189990	230776302876210	230776302876210	307701742379850	384627181883490
	u	76925445343110	230776324350390	230776324350390	307701742379850	384627160409310
6	g	105558839695238	316676372282498	316676372282498	422235168731122	527793965116762
	u	105558766325122	316676359159388	316676359159388	422235168731122	527793978239872
5	g	132192048566407	396576257904751	396576257904751	528768349717375	660960441593380
	u	132192104637877	396576288326506	396576288326506	528768349717375	660960411171626
4	g	149756135192451	449268209006409	449268209006409	599024284319331	748780359631857
	u	149756036906781	449268187532229	449268187532229	599024284319331	748780381106037
3	g	150988575234761	452965890255683	452965890255683	603954525370369	754943160401075
	u	150988657552451	452965927697843	452965927697843	603954525370369	754943122958915
2	g	130959602829132	392878578569538	392878578569538	523838108687332	654797638889108
	u	130959487828212	392878548147782	392878548147782	523838108687332	654797669310862
1	g	89413675311916	268241236547900	268241236547900	357654984571154	447068732594408
	u	89413780617992	268241276664500	268241276664500	357654984571154	447068692477808

These results have errors. See Errata pages for correct spin weight

Errors are so small that Fig. 3 is not affected.

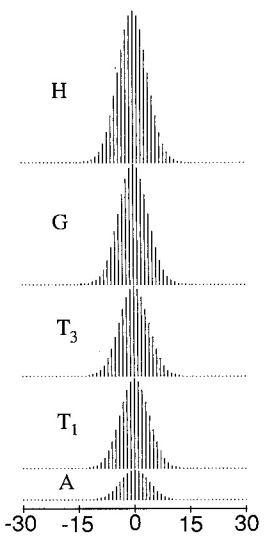

Fig. 3. Case 1 hyperfine multiplets for $^{13}C_{60}$. Nuclear spin states corresponding to $I > 15$ are in an increasingly tiny minority. They are indicated by dots in the wings of the hyperfine splitting distributions.

that any sum over I does also. The total nuclear spin weights according to Y_h and Y species are shown in table 2. One notes that most of the spin states come in parity doublets. However, most of the species have slightly differing numbers of odd (u) and even (g) states. Only G_g and G_u match inversion doublets perfectly.

Table 2

A_g	$9.607680278974464000\times10^{15}$
T_{1g}	$2.882303707830067200\times10^{16}$
T_{3g}	$2.882303707830067200\times10^{16}$
G_g	$3.843071682040217600\times10^{16}$
H_g	$4.803839656198144000\times10^{16}$
A_u	$9.607678399926272000\times10^{15}$
T_{1u}	$2.882303788360704000\times10^{16}$
T_{3u}	$2.882303788360704000\times10^{16}$
G_u	$3.843071682040217600\times10^{16}$
H_u	$4.803839575667507200\times10^{16}$

4. Superhyperfine structure

Heretofore the simplest case (case 1) has been assumed in which each icosahedral species {A, T_1, T_3, G, H} is a good quantum label of the rotational fine structure and total nuclear spin $\{I+0, 1, ..., 30\}$ is a good quantum for hyperfine structure. This neglects the inevitable superfine structure that arises when the rotational quantum number R or N is high. Then the superfine splitting becomes much smaller than the hyperfine splitting and allows different species and I states in a cluster to mix strongly through tensor spin rotations interactions which otherwise would have negligible effects.

The case in which nuclear spin and rotational states mix is called case 2. The transition between case 1 and case 2 is analogous in some ways to the transition between LS coupling and jj coupling in shell theory. Breakdown of superfine and hyperfine structure into superhyperfine patterns has been identified in the very highest resolution spectra of SF_6 [18,19]. They show that one of its symmetry axes becomes a permanent axis of rotation and the feasible symmetry reduces to the local subgroup associated with that axis. This is an example of spontaneous symmetry breaking.

When rotational symmetry is broken the effective or "feasible" permutational symmetry is reduced, as well. Previously equivalent nuclear positions become distinguished by their positions relative to the rotational axis. Rotationally induced "chemical shifts"split the hyperfine spectra into patterns that are analogous to NMR patterns. Discussion of the possible superhyperfine patterns in $^{13}C_{60}$ will be given in subsequent works.

Acknowledgement

We would like to thank the Theoretical and Computational Chemistry division of the National Science Foundation for support on grant CHM 89-16787. We would also like to thank Robert W. Hellwarth and the 22nd Winter Colloquium on Quantum Electronics for stimulation and encouragement in connection with this work.

References

[1] H.W. Kroto, J.R. Heath, S.C. O'Brien, R.F. Curl and R.E. Smalley, Nature 318 (1985) 162.
[2] D.M. Cox, D.J. Trevor, K.C. Reichmann and A. Kaldor, J. Am. Chem. Soc. 108 (1986) 2457.
[3] W. Krätschmer, K. Fostiropoulos and D.R. Huffman, in: Dusty objects in the universe, eds. E. Bussoletti and A.A. Vittone (Kluwer, Dordrecht, 1990); Chem. Phys. Letters 170 (1990) 167.
[4] D.E. Weeks and W.G. Harter, Chem. Phys. Letters 144 (1988) 366;
R.E. Stanton and M.D. Newton, J. Phys. Chem. 92 (1988) 2141.
[5] W. Krätschmer, L.D. Lamb, K. Fostiropoulos and D.R. Huffman, Nature 347 (1990) 354.
[6] D.S. Bethune, G. Meijer, W.C. Tang and H.J. Rosen, Chem. Phys. Letters 174 (1990) 219.
[7] R.D. Johnson, G. Meijer and D.S. Bethune, J. Am. Chem. Soc. 112 (1990) 8983.
[8] J.M. Hawkins, A. Meyer, T.A. Lewis, S.D. Loren and F.J. Hollander, Science 252 (1991) 312.
[9] R.J. Wilson, D.S. Bethune, R.D. Johnson, D.D. Chambliss, M.S. DeVries and H.E. Humziker, Nature 348 (1990) 621.
[10] W. Krätschmer and D.R. Huffman, Nature 348 (1990) 623.
[11] C.I. Frum, R. Engleman Jr., H.G. Hedderich, P.F. Bernmath, L.D. Lamb and D.R. Huffman, Chem. Phys. Letters 170 (1990) 167.
[12] W.G. Harter and D.E. Weeks, Chem. Phys. Letters 132 (1986) 387.
[13] W.G. Harter and D.E. Weeks, J. Chem. Phys. 90 (1989) 4727.
[14] D.E. Weeks and W.G. Harter, J. Chem. Phys. 90 (1989) 4772.
[15] D.E. Weeks and W.G. Harter, Chem. Phys. Letters 176 (1991) 209.
[16] W.G. Harter, Phys. Rev. A 24 (1981) 192.
[17] W.G. Harter, E.W. Patterson and F.J. daPaixao, Rev. Mod. Phys. 50 (1978) 37.
[18] J. Bordé and Ch.J. Bordé, Chem. Phys. 71 (1982) 417.
[19] W.G. Harter, in: Proceedings of the XVth Colloquium on Group theoretical methods in physics, ed. R. Gilmore (World Scientific, Singapore, 1986) p. 1.
[20] W.G. Harter and C.W. Patterson, Lecture notes in physics, No. 49 (Springer, Berlin, 1976); Phys. Rev. A 13 (1976) 1067.
[21] W.G. Harter, Phys. Rev. A 8 (1973) 2819.

Errata: Nuclear spin weights and gas phase spectral structure of $^{12}C_{60}$ and $^{13}C_{60}$ Buckminsterfullerene

William G. Harter
and
Tyle C. Reimer

University of Arkansas
Fayetteville, AR 72701

Erratum

The correlation table between S_{60} and Y_h representations contain small errors, generally in the sixth or seventh place of the observable distribution. Errors of one part in 10^6 do not affect the predictions for spectral intensity distributions in the figures and would normally be unobservable. However, the errors are significant with regard to the tiny populations of states of highest spin, should they become important in some future experiment. The revised correlations (Table 1) are given below. Numerical changes are required in the section entitled: Spin permutation Symmetry of $^{13}C_{60}$. On page 235, the third sentence in paragraph 7 should be changed to read:

Neither A_g nor A_u has an (I = 29) multiplet but they have 22 and 14 (I = 28) multiplets, respectively.

On page 235, the third sentence in paragraph 8 should read as:

Then the numbers of states begin to level off and attain a maximum value of about seven hundred and fifty trillion for H_u or H_g species having nuclear spin I = 3 and 4.

The total nuclear spin weights on page 237, should be revised as follows :

A_g	9.607679885269312000e+15
T_{1g}	2.882303697092649600e+16
T_{3g}	2.882303697092649600e+16
G_g	3.843071685619372800e+16
H_g	4.803839674093824000e+16
A_u	9.607678793631424000e+15
T_{1u}	2.882303799098121600e+16
T_{3u}	2.882303799098121600e+16
G_u	3.843071678461062400e+16
H_u	4.803839557771827200e+16

Finally, all species have slightly differing weights for odd and even parity. The G species are not exceptional in this regard; hence, the final sentence on page 237 should be omitted.

I	Par	A	T_1	T_3	G	H
30	g	1	0	0	0	0
	u	0	0	0	0	0
29	g	0	1	1	2	3
	u	0	2	2	2	2
28	g	22	36	36	58	80
	u	14	42	42	56	70
27	g	280	804	804	1084	1354
	u	260	826	826	1086	1336
26	g	3887	11238	11238	15125	19022
	u	3772	11324	11324	15096	18878
25	g	41528	124257	124257	165779	207307
	u	41266	124548	124548	165808	207074
24	g	372752	1114158	1114158	1486916	1859568
	u	371694	1114942	1114942	1486642	1858246
23	g	2801748	8402852	8402852	11204600	14006448
	u	2799558	8405316	8405316	11204874	14004522
22	g	18110340	54304371	54304371	72414711	90525051
	u	18103410	54309474	54309474	72412884	90516294
21	g	101874363	305608974	305608974	407483337	509357130
	u	101861196	305623968	305623968	407485164	509345790
20	g	505125708	1515241704	1515241704	2020367376	2525493654
	u	505090980	1515266928	1515266928	2020357878	2525449428
19	g	2227563126	6682635360	6682635360	8910198522	11137761648
	u	2227502850	6682705140	6682705140	8910208020	11137710870
18	g	8805633300	26416344630	26416344630	35221977930	44027608785
	u	8805495420	26416442910	26416442910	35221938330	44027431350
17	g	31395905685	94187559795	94187559795	125583465480	156979373610
	u	31395687300	94187817780	94187817780	125583505080	156979194780
16	g	101492436960	304475471640	304475471640	405967908600	507460345560
	u	101491992360	304475780520	304475780520	405967772880	507459765240
15	g	298734989924	896204629630	896204629630	1194939619444	1493674601616
	u	298734348764	896205406510	896205406510	1194939755164	1493674096176
14	g	803453709856	2410356037985	2410356037985	3213809747951	4017263465559
	u	803452525816	2410356831830	2410356831830	3213809357756	4017261891324
13	g	1980110898945	5940332333550	5940332333550	7920443232495	9900554131440
	u	1980109351620	5940334271070	5940334271070	7920443622690	9900552974310
12	g	4481735502630	13445194549380	13445194549380	17926930052010	22408665535200
	u	4481732871390	13445196226770	13445196226770	17926929098160	22408661950230
11	g	9331438352730	27994315570980	27994315570980	37325753923710	46657192295880
	u	9331435261110	27994319616450	27994319616450	37325754877560	46657190157990
10	g	17892025439775	53676052490265	53676052490265	71568077929785	89460103369560
	u	17892020535870	53676055391160	53676055391160	71568075926790	89460096462660
9	g	31605175642230	94815530686980	94815530686980	126420706329465	158025881932935
	u	31605170531130	94815537801090	94815537801090	126420708332460	158025878824830
8	g	51415130846760	154245351765540	154245351765540	205660482612300	257075613497820
	u	51415123186380	154245355784100	154245355784100	205660478970480	257075602195620
7	g	76925432220000	230776308338940	230776308338940	307701740558940	384627172778940
	u	76925425313100	230776318887660	230776318887660	307701744200760	384627169513860
6	g	105558807981090	316676363633175	316676363633175	422235171614265	527793979532265
	u	105558798039270	316676367808710	316676367808710	422235165847980	527793963824370
5	g	132192080280555	396576266554074	396576266554074	528768346834233	660960427177878
	u	132192072923730	396576279677184	396576279677184	528768352600518	660960425587128
4	g	149756091280506	449268197030424	449268197030424	599024288311326	748780379591832
	u	149756080818726	449268199508214	449268199508214	599024280327336	748780361146062
3	g	150988619146706	452965902231668	452965902231668	603954521378374	754943140441100
	u	150988613640506	452965915721858	452965915721858	603954529362364	754943142918890
2	g	130959549507485	392878564027270	392878564027270	523838113534755	654797663126220
	u	130959541149860	392878562690050	392878562690050	523838103839910	654797645073750
1	g	89413728633564	268241251090167	268241251090167	357654979723731	447068708357295
	u	89413727296344	268241262122232	268241262122232	357654989418576	447068716714920
0	g	31791575566072	95374646372040	95374646372040	127166221937640	158957797411208
	u	31791571643468	95374639953380	95374639953380	127166211596396	158957783147612

Table 1. Frequency table relating the number of Y_h species { A_g,T_{1g}, T_{3g}, G_g, H_g, A_u,T_{1u}, T_{3u}, G_u, H_u } that correlate with each of the S_{60} permutation group species. The g and u characters in the parity column denote even and odd parity respectively, and the I column labels each of the pertinent S_{60} species by total nuclear spin.

I	Par	A	T_1	T_3	G	H
30	g	1	0	0	0	0
	u	0	0	0	0	0
29	g	0	1	1	2	3
	u	0	2	2	2	2
28	g	22	36	36	58	80
	u	14	42	42	56	70
27	g	280	804	804	1084	1354
	u	260	826	826	1086	1336
26	g	3887	11238	11238	15125	19022
	u	3772	11324	11324	15096	18878
25	g	41528	124257	124257	165779	207307
	u	41266	124548	124548	165808	207074
24	g	372752	1114158	1114158	1486916	1859568
	u	371694	1114942	1114942	1486642	1858246
23	g	2801748	8402852	8402852	11204600	14006448
	u	2799558	8405316	8405316	11204874	14004522
22	g	18110340	54304371	54304371	72414711	90525051
	u	18103410	54309474	54309474	72412884	90516294
21	g	101874363	305608974	305608974	407483337	509357130
	u	101861196	305623968	305623968	407485164	509345790
20	g	505125708	1515241704	1515241704	2020367376	2525493654
	u	505090980	1515266928	1515266928	2020357878	2525449428
19	g	2227563126	6682635360	6682635360	8910198522	11137761648
	u	2227502850	6682705140	6682705140	8910208020	11137710870
18	g	8805633300	26416344630	26416344630	35221977930	44027608785
	u	8805495420	26416442910	26416442910	35221938330	44027431350
17	g	31395905685	94187559795	94187559795	125583465480	156979373610
	u	31395687300	94187817780	94187817780	125583505080	156979194780
16	g	101492436960	304475471640	304475471640	405967908600	507460345560
	u	101491992360	304475780520	304475780520	405967772880	507459765240
15	g	298734989924	896204629630	896204629630	1194939619444	1493674601616
	u	298734348764	896205406510	896205406510	1194939755164	1493674096176
14	g	803453709856	2410356037985	2410356037985	3213809747951	4017263465559
	u	803452525816	2410356831830	2410356831830	3213809357756	4017261891324
13	g	1980110898945	5940332333550	5940332333550	7920443232495	9900554131440
	u	1980109351620	5940334271070	5940334271070	7920443622690	9900552974310
12	g	4481735502630	13445194549380	13445194549380	17926930052010	22408665535200
	u	4481732871390	13445196226770	13445196226770	17926929098160	22408661950230
11	g	9331438352730	27994315570980	27994315570980	37325753923710	46657192295880
	u	9331435261110	27994319616450	27994319616450	37325754877560	46657190157990
10	g	17892025439775	53676052490265	53676052490265	71568077929785	89460103369560
	u	17892020535870	53676055391160	53676055391160	71568075926790	89460096462660
9	g	31605175642230	94815530686980	94815530686980	126420706329465	158025881932935
	u	31605170531130	94815537801090	94815537801090	126420708332460	158025878824830
8	g	51415130846760	154245351765540	154245351765540	205660482612300	257075613497820
	u	51415123186380	154245355784100	154245355784100	205660478970480	257075602195620
7	g	76925432220000	230776308338940	230776308338940	307701740558940	384627172778940
	u	76925425313100	230776318887660	230776318887660	307701744200760	384627169513860
6	g	105558807981090	316676363633175	316676363633175	422235171614265	527793979532265
	u	105558798039270	316676367808710	316676367808710	422235165847980	527793963824370
5	g	132192080280555	396576266554074	396576266554074	528768346834233	660960427177878
	u	132192072923730	396576279677184	396576279677184	528768352600518	660960425587128
4	g	149756091280506	449268197030424	449268197030424	599024288311326	748780379591832
	u	149756080818726	449268199508214	449268199508214	599024280327336	748780361146062
3	g	150988619146706	452965902231668	452965902231668	603954521378374	754943140441100
	u	150988613640506	452965915721858	452965915721858	603954529362364	754943142918890
2	g	130959549507485	392878564027270	392878564027270	523838113534755	654797663126220
	u	130959541149860	392878562690050	392878562690050	523838103839910	654797645073750
1	g	89413728633564	268241251090167	268241251090167	357654979723731	447068708357295
	u	89413727296344	268241262122232	268241262122232	357654989418576	447068716714920
0	g	31791575566072	95374646372040	95374646372040	127166221937640	158957797411208
	u	31791571643468	95374639953380	95374639953380	127166211596396	158957783147612

Table 1. Frequency table relating the number of Y_h species { A_g,T_{1g}, T_{3g}, G_g, H_g, A_u,T_{1u}, T_{3u}, G_u, H_u } that correlate with each of the S_{60} permutation group species. The g and u characters in the parity column denote even and odd parity respectively, and the I column labels each of the pertinent S_{60} species by total nuclear spin.